RI 9463

REPORT OF INVESTIGATIONS/1993

Thermal Modeling of Portable Power Cables

By Michael R. Yenchek, Gregory P. Cole, and John C. Edwards

UNITED STATES DEPARTMENT OF THE INTERIOR

BUREAU OF MINES

Report of Investigations 9463

Thermal Modeling of Portable Power Cables

By Michael R. Yenchek, Gregory P. Cole, and John C. Edwards

UNITED STATES DEPARTMENT OF THE INTERIOR
Bruce Babbitt, Secretary

BUREAU OF MINES

Library of Congress Cataloging in Publication Data:

Yenchek, M. R. (Michael R.)
Thermal modeling of portable power cables / by Michael R. Yenchek, Gregory P. Cole, and John C. Edwards.

p. cm. — (Report of investigations / United States Department of the Interior, Bureau of Mines; 9463)

Includes bibliographical references (p. 14).

1. Coal mining machinery—Electric equipment—Protection. 2. Electric cables—Thermal properties—Mathematical models. 3. Electric currents—Heating effects—Mathematical models. I. Cole, Gregory P. II. Edwards, John C. III. Title. IV. Series: Report of investigations (United States. Bureau of Mines); 9463.

TN23.U43 [TN813] 622 s—dc20 [622'.334] 92-44394 CIP

CONTENTS

ILLUSTRATIONS

TABLES

UNIT OF MEASURE ABBREVIATIONS USED IN THIS REPORT

A	ampere	e	irrational constant approximately equal to 2.71828...
°C	degree Celsius	fps	foot per second
cal/(cm•s)	calorie per centimeter per second	ft	foot
cal/(cm•s•K)	calorie per centimeter per second per kelvin	g/cm^3	gram per cubic centimeter
$cal/(cm^2•s•K)$	calorie per square centimeter per second per kelvin	h	hour
$cal/(cm^2•s•K^4)$	calorie per square centimeter per second per kelvin to the fourth power	in	inch
cal/(g•K)	calorie per gram per kelvin	K	kelvin
cm	centimeter	min	minute
cmil	circular mil	Ω	ohm
		Ω-cm	ohm-centimeter
		s	second

THERMAL MODELING OF PORTABLE POWER CABLES

By Michael R. Yenchek,[1] Gregory P. Cole,[2] and John C. Edwards[3]

ABSTRACT

The U.S. Bureau of Mines investigated the performance of portable power cables under transient conditions. This research had a twofold purpose: (1) to define the thermal characteristics of electrically overloaded trailing cables, and (2) to conceptualize electrical protection for cables that allows maximum cable efficiency without diminishing electrical safety in underground mines. Several tasks were undertaken in support of these goals during the 3-year research effort. Overload tests ranging from 2 to 12 times rated ampacity were conducted in the Bureau's Mine Electrical Laboratory. Two thermal models of energized type G-GC trailing cables were constructed, one based on thermodynamic theory and the other using empirical data from previous Bureau load tests. The empirical model was then incorporated into an interactive computer program that can assist designers and approvers of mining machines in selecting the appropriate size trailing cable. This program can be the basis for a cable protection system that ensures that cables are not the source of fires, ignitions, burns, or explosions underground.

[1]Electrical engineer.
[2]Computer engineer.
[3]Research physicist.
U.S. Bureau of Mines, Pittsburgh Research Center, Pittsburgh, PA.

INTRODUCTION

Extreme mechanical abuse of hardware is characteristic of mobile equipment operation in underground coal mines, so much so that trailing cables rarely last a year in this environment (*1*).[4] Abrasive, tensile, and crushing forces can cause phase-to-phase and phase-to-ground faults and ultimate cable failure when circuit protective devices are inadequate. The energy expended in a trailing cable short circuit is capable of igniting loose coal and coal dust on a mine floor as well as an explosive mixture of methane and air. In addition, combustion of the cable insulation can create smoke and noxious fumes. When sustained, even overload currents only slightly in excess of the rated cable ampacity can expose personnel handling the cable to burn hazards, and enhance thermal degradation of the insulation and jacket.

Effective cable protection can lessen such potential dangers in the underground environment by ensuring that the cable is operated within safe limits that preclude injury to personnel and damage to the cable itself. This protection should also ensure that the cable is electrically utilized in an efficient manner. To accomplish this, the protection must account for all aspects of cable operation. Device response time and sensitivity should be based upon cable performance, not only during overloads and short circuits, but also under continuous and intermittent duty. A prerequisite for the implementation of such protection is a comprehensive understanding of the thermal characteristics of energized cables. In cooperation with the Mine Safety and Health Administration (MSHA), the American Mining Congress (AMC), and the Insulated Cable Engineers Association (ICEA), the U.S. Bureau of Mines conducted research to define the relationship between current load and resultant temperature rise in trailing cables loaded continuously and intermittently under normal circumstances (*2-3*). Cable characteristics under abnormal or faulted conditions remained to be investigated, however.

This report documents the accomplishments of a follow-up Bureau research project supporting the Bureau's goal of enhancing the safety of the Nation's underground miners. The specific objectives of this project were (1) to define the thermal characteristics of electrically overloaded trailing cables, and (2) to conceptualize electrical protection for cables that allows maximum cable efficiency without diminishing electrical safety in underground mines. The principal product of this work is a computerized thermal model that can assist designers and approvers of mining machines in selecting the appropriate size trailing cable. The authors recognize there are other concerns associated with mine trailing cable operation that are beyond the scope of this document. They are noted in the "Recommendations for Future Research" section.

BACKGROUND

The performance of copper conductor cables under short circuit has been well established for many years (*4*) and may be expressed as

$$\left(\frac{I}{A}\right)^2 t F_{ac} = 0.0297 \log_{10} \frac{T_f + 234}{T_i + 234}, \qquad (1)$$

where I = short circuit current, A,

A = conductor area, cmil,

t = short circuit duration, s,

F_{ac} = skin effect or ac/dc ratio,

T_f = final conductor temperature after a change in current, °C,

and T_i = conductor temperature prior to a change in current, °C.

This equation is the basis of present ICEA specifications for short circuited insulated cables (*5-6*). This equation assumes that heat transfer from the conductor is negligible, a valid assumption for short time periods (*7*). However, for fault durations greater than several seconds, conduction and radiation become significant, increasing the error in application of this assumption.

The intermediate time zone from 10 s up to 6 h is the bridge between short circuit performance and continuous duty. The Institute of Electrical and Electronic Engineers (IEEE) Buff Book (*8*) calls this region "the greatest unknown in the cable thermal characteristic." Emergency overload ratings have been established for medium-voltage cables (*9*), but their applicability to low-voltage portable power cables is uncertain. In previous Bureau research (*10*), the relationship between cable thermal life and temperature was determined through accelerated life testing. In addition, the impact of current loads on this thermal life was mathematically derived for normal machine loads (*11*).

[4]Italic numbers in parentheses refer to items in the list of references preceding the appendix at the end of this report.

Further laboratory investigations of cable transient performance were necessary to quantify the thermal effects of fault currents and to incorporate those effects into the time-current characteristics of effective cable protection.

Short circuit protection of trailing cables in coal mines is presently required by Federal regulation (*12*). This protection typically involves the activation of a dual-element fuse or molded-case circuit breaker with no intentional time delay. The trip settings specified by Federal regulations are based upon available fault currents and cable size. Higher trip levels may be permitted when nuisance tripping results from motor starting or transformer magnetizing currents (*13-14*).

However, protection of cables against overloads and lower current, higher resistance arcing faults is not mandated by Federal law. The absence of this regulatory impetus means that many cables can be vulnerable to severe damage over a significant portion of their operating range. Indeed, Luxbacher (*15*), in discussions with mine operators, found that even circuit breakers equipped with thermal overload protection rarely tripped during these faults. Yet it is not uncommon to see cables that have been damaged by relatively low-level overcurrents. A protection scheme accurately tuned to cable damage limits can obviate such occurrences.

ACKNOWLEDGMENT

The authors acknowledge with thanks the assistance provided by Dr. William Z. Black of Technology, Inc., Atlanta, GA, who helped interpret the laboratory test results from a thermodynamic standpoint.

CABLE PROTECTION CONCEPTS

An effective cable protection system allows the cable to be operated within the limits of its thermal capability while precluding conduction of unsafe load currents. Hazardous combinations of current and time, in the long term, can thermally degrade the cable insulation and jacket. In the short term, they can ignite loose coal dust or methane accumulations. Several approaches to cable protection had been envisioned at the outset of the project, each having advantages and drawbacks. The primary consideration was identification of the appropriate parameter to be sensed, i.e., cable temperature or load current.

Originally, temperature monitoring was favored as it provides a direct measure of the cable's thermal history. Thermocouples, thermistors, and resistance temperature detectors were under consideration as temperature sensors that could be embedded within the metallic conductor. Ideally, this cable temperature monitor should be installed in the same environment as the cable. The main drawback in having the sensor in open air, underground, is its susceptibility to physical damage. The load center from which the trailing cable originates can provide the necessary mechanical protection. Also, in the load center the recommended cable protection system would logically be near other electrical protective devices such as ground monitors. Ambient compensation could even be incorporated to account for the elevated temperatures within this enclosure. However, no practical means could be found to compensate for the thermal influence of nearby cable terminations or end effects that would distort cable temperature data (*2*). Consequently, development of the cable protection concept using temperature monitoring was abandoned in favor of the traditional approach of load current sensing.

Load currents can be measured with a current transformer (CT) that encircles a power conductor. Cable temperatures can then be inferred from the output signal of the CT secondary. The success of this methodology depends upon how accurately temperature fluctuations can be predicted or modeled. In the course of this research two thermal models of energized type G-GC trailing cables were constructed, one based on thermodynamic theory and the other using empirical data from previous Bureau load tests (*2*).

MATHEMATICAL MODEL

A mathematical model was developed that predicts the transient heating and cooling of *round*, type G-GC trailing cables suspended in open air. The cable features n copper conductors (n = 2 or 3, typically) of radius R_w. Each conductor is covered by insulation, a dielectric material such as ethylene-propylene-rubber (EPR) or polychloroprene (neoprene). The insulated conductors are embedded in a solid cable jacket material such as chlorosulfonated polyethylene or neoprene for mechanical protection.

Thermal production of heat occurs in the conductor as the result of electrical current through a small, nonzero resistance. Symmetry with respect to a longitudinal axis, at the cable center and parallel to the cable, results in the radial transport of thermal energy to the outer surface of the cable jacket, where the energy is lost to the external environment (air) through free convection and radiation. The proper description of heat generation and heat dissipation results in a thermal transport equation that can be solved for the temperature over the cross section of the cable at any time. The presence of several conductors within the cable creates a complex geometry for the exact analytic representation of the current and heat flow within the cable. However, the near symmetry of the conductors about the cable longitudinal axis permits the representation of the n conductors by a single conductor of equivalent cross-sectional area in order to define a boundary surface of radius R_o for the heat generation source of n wires. A simple geometric equivalence of wire cross-sectional area defines R_o as

$$R_o = \sqrt{n} \times R_w, \tag{2}$$

where R_o = radius of boundary surface of conductors, cm,

n = number of conductors,

and R_w = conductor radius, cm.

Surrounding the equivalent-heat-generating cylindrical element of radius R_o is an insulation of radius R_1 with respect to the central axis. Concentric with the equivalent-heat-generating element is a cable jacket of radius R_2. A schematic of the equivalent cable cross section is shown in figure 1.

Each wire of electrical resistivity ρ (ohm-centimeters) contributes to the total heat conduction rate S for uniform current I (amperes).

$$S = \frac{\left(n \times \rho \times I^2\right)}{\left(4.184 \times \pi \times R_w^2\right)}, \tag{3}$$

where S = heat conduction rate, cal/(cm•s),

ρ = electrical resistivity, Ω-cm,

I = electrical current, A,

and π = 3.14159265.

For a cable length, l, the appropriate heat transport equation for radial heat flow defines a partial differential equation for the temperature $T_1(t)$ of the region $r < R_o$ at time t,

$$l\pi R_o^2 \sigma_1 C_{p_1} \frac{dT_1}{dt} = lS - 2\pi R_o l \lambda_2 \frac{\partial T_2}{\partial r}\Big|_{R_o}, \tag{4}$$

where l = cable length, cm,

σ_1 = conductor mass density, g/cm^3,

C_{p_1} = conductor specific heat, cal/(g•K),

T_1 = conductor temperature, K,

T_2 = insulation temperature, K,

λ_2 = insulation thermal conductivity, cal/(cm•s•K),

t = time, s,

and r = radial distance from longitudinal axis of cable, cm.

The second term on the right side of equation 4 represents the conductive loss of thermal energy into the insulation surrounding the conductor. Equation 4 is based upon the model assumption that the conductor's high thermal conductivity rapidly establishes a uniform temperature over the conductor. Equation 4 is simplified to read

$$\sigma_1 C_{p_1} \frac{dT_1}{dt} = \frac{S}{\pi R_o^2} - \frac{2}{R_o} \lambda_2 \frac{\partial T_2}{\partial r}\Big|_{R_o}. \tag{5}$$

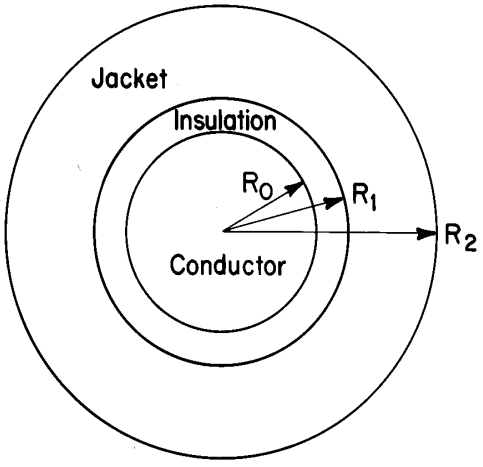

Figure 1.—Equivalent cable cross section for mathematical model.

The heat transport equations appropriate for the insulation and cable jacket differ only in the thermal properties of the materials. Because of the much slower thermal diffusion of the insulation and cable jacket, the thermal conduction within these materials has to be considered explicitly. The thermal transport equation for these regions is written in condensed notation in terms of the local temperature $T_k(r,t)$,

$$\sigma_k C_{p_k} \frac{\partial T_k}{\partial t} = \lambda_k \left(\frac{\partial^2 T_k}{\partial r^2} + \frac{1}{r} \frac{\partial T_k}{\partial r} \right), \qquad (6)$$

where σ_k = mass density of material k, g/cm^3,

C_{p_k} = specific heat of material k, cal/(g•K),

λ_k = thermal conductivity of material k, cal/(cm•s•K),

T_k = temperature of material k, K,

k = 2 for insulation,

and k = 3 for jacket.

The right side of equation 6 is based upon cylindrical symmetry. Equations 5 and 6 are written in dimensionless form as

$$\frac{d\theta_1}{du} = \frac{\tau_1}{T_o} \frac{1}{\sigma_1 C_{p_1}} \frac{S}{\pi R_o^2} - \frac{2}{R_o^2} \frac{\lambda_2}{\sigma_1 C_{p_1}} \tau_1 \frac{\partial \theta_2}{\partial y}\Big|_{y=1}, \qquad (7)$$

and

$$\frac{\partial \theta_k}{\partial u} = P_k \left(\frac{\partial^2 \theta_k}{\partial y^2} + \frac{1}{y} \frac{\partial \theta_2}{\partial y} \right), \qquad (8)$$

where $u = t/\tau_1$,

$y = r/R_o$,

$\theta_k = T_k/T_o$,

$\tau_k = R_o^2 \sigma_k C_{pk}/\lambda_k$,

and $P_k = \tau_1/\tau_k$.

Equations 7 and 8 are solvable in principle if specified initial conditions and boundary conditions are available. The initial condition is that the cable is at ambient temperature. The boundary conditions are written in the form of dimensionless material temperature.

(i) $$\lambda_1 \frac{\partial \theta_1}{\partial y} = \lambda_2 \frac{\partial \theta_2}{\partial y} @ y = 1, \qquad (9)$$

(ii) $$\lambda_2 \frac{\partial \theta_2}{\partial y} = \lambda_3 \frac{\partial \theta_3}{\partial y} @ y = \frac{R_1}{R_o}, \qquad (10)$$

(iii) $$\frac{\lambda_3}{R_o} \frac{\partial \theta_3}{\partial y} = h(\theta_3 - 1) + \sigma \epsilon T_o^3 (\theta_3^4 - 1) @ y = \frac{R_2}{R_o}, \qquad (11)$$

where h = convective heat transfer coefficient, $cal/(cm^2 \cdot s \cdot K)$,

σ = Stefan-Boltzmann radiation constant, 1.355×10^{-12} $cal/(cm^2 \cdot s \cdot K^4)$,

ϵ = jacket emissivity (absorptivity),

T_o = ambient temperature, K.

Conditions (i) and (ii) state that a continuity of heat flow occurs where the materials are in contact. Condition (iii) defines the heat loss at the jacket surface due to free convection and radiation.

The free convection heat transfer coefficient h is defined in terms of the temperature difference between the jacket surface and ambient air, $T_3(R_2) - T_o$, (*15*),

$$h = \frac{1}{4.184} 7.72506 \times 10^{-4} \left[\frac{(T_3(R_2)) - T_o}{(2R_2)} \right]^{0.25}. \qquad (12)$$

The partial differential equations 7 and 8 and associated boundary conditions must be solved with a numerical procedure. A finite difference method that is implicit in time and central in space was selected to reduce the partial differential equations to a set of coupled algebraic equations that could be solved iteratively at each step with a Gaussian elimination method (*16*). A FORTRAN computer program was developed to solve these algebraic equations. The program has the flexibility to solve each particular application for a known set of physical properties characteristic of the cable.

Physical specifications for EPR insulation and neoprene jackets were obtained from cable manufacturers and used in the model calculations (table 1).

Table 1.—Physical data

Property	Conductor	EPR	Neoprene
Mass density .... g/cm^3 ..	8.96	1.35	1.5
Specific heat .. cal/(g•K) ..	0.092	0.393	0.335
Thermal conductivity cal/(cm•s•K) ..	0.96	6.62 x 10^{-4}	6.62 x 10^{-4}

Calculations were made for two sizes of round, 3/C, G-GC cables, #2/0 and #4/0 AWG. Dimensions and wire resistances are listed in table 2.

Table 2.—Cable dimensions and wire resistance

Property	#2/0 AWG, round G-GC	#4/0 AWG, round G-GC
Wire diameter ..... in ..	0.419	0.528
Insulation thickness .. in ..	0.08	0.08
Jacket diameter ..... in ..	1.65	2.04
Wire resistance ohm per 1,000 ft ..	0.101	0.0626

AWG American wire gauge.

Figures 2 and 3 show the calculated temperatures above ambient (20° C) at y = 1, R_1/R_o, and R_2/R_o, of the #2/0 and #4/0 cables for a constant wire current of 400 A. The temperatures of the wire (conductor), insulation-jacket interface, and jacket external surface all reach a steady state value within a 2-h time period.

Table 3 shows a comparison of measured and predicted steady state wire temperature rises above ambient for currents of 100, 200, and 400 A in each cable. There is a reasonable agreement between measured and predicted values. Discrepancies are quite possibly due to the inexact definition of the free convective cable-air heat transfer coefficient. This, and the radiation boundary condition, are temperature dependent. Their influence is seen from

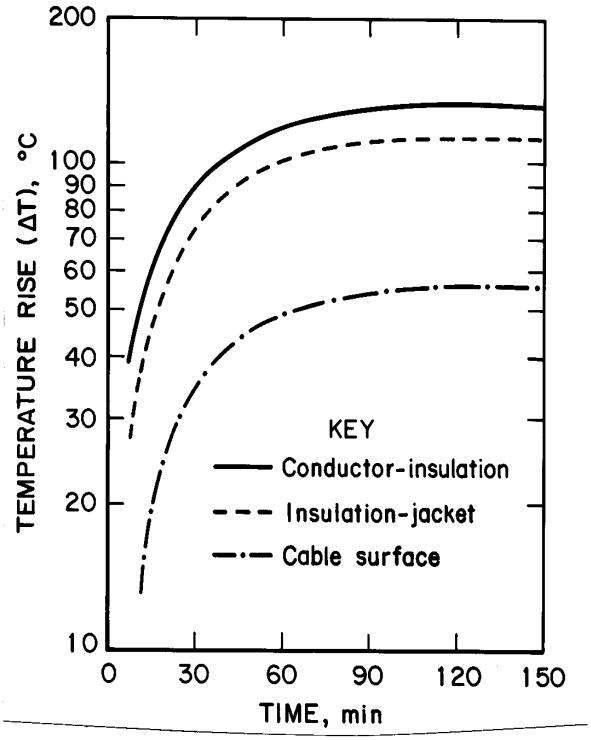

Figure 2.—Mathematical model predicted temperature rise in #2/0 AWG, 3/C, round, G-GC cable loaded at 400 A.

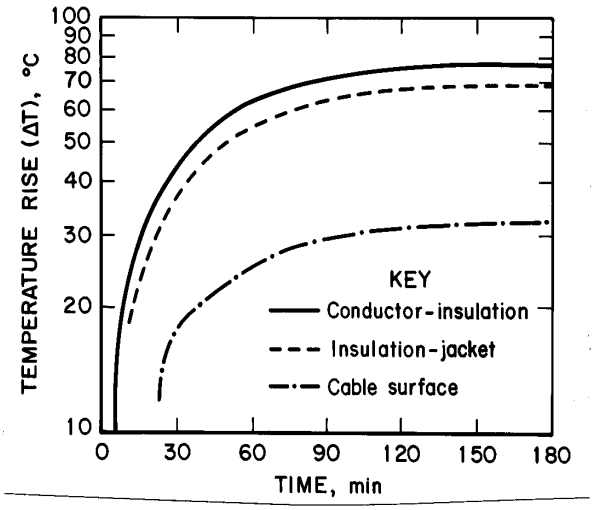

Figure 3.—Mathematical model predicted temperature rise in #4/0 AWG, 3/C, round, G-GC cable loaded at 400 A.

a comparison of the rise time for the conductor temperature rise above ambient to reach e^{-1} of the maximum temperature rise above ambient. For a #2/0 AWG, 3/C cable, calculations with an isothermal boundary condition at

the jacket surface yielded a rise time of 4.6 min for wire currents of 100, 200, 400, and 800 A. For the #2/0 AWG, 3/C case reported in table 3, the rise time is 30.4 min for currents of 100 and 200 A. For a 400-A current, the rise time is 26.6 min. The temperature dependence in the jacket boundary condition causes the rise time to (1) differ from the isothermal boundary condition case, and (2) vary with the heat production rate (wire current).

Table 3.—Measured and predicted wire temperature rises

Cable, 3/C, round G-GC	Current, A	Stabilized wire temperature rise, °C	
		Measured (2)	Model prediction
#2/0 AWG ..	100	8	10
	200	28	37
	400	128	132
#4/0 AWG ..	100	8	6
	200	20	22
	400	68	79

The FORTRAN program developed has the capability to impose a duty cycle on the current. An example is presented in figure 4. Figure 4 represents the evolution of the temperature rise above ambient for a #4/0 AWG, 3/C, round cable subjected to a maximum current of 800 A with a 25% duty cycle for a 50.4-min period.

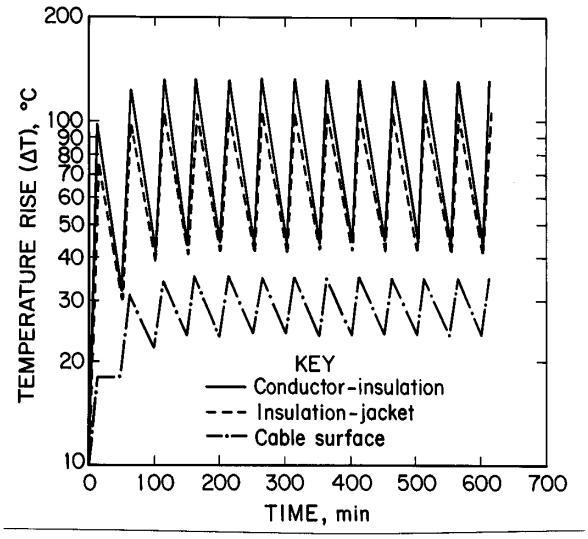

Figure 4.—Mathematical model predicted temperature rise in #4/0 AWG, 3/C, round, G-GC cable loaded at 800 A, 25% of the time.

EMPIRICAL MODEL

Concurrent with the theoretical analysis, a thermal model empirically based on laboratory test results was constructed for 3/C, G-GC trailing cables suspended in open air. The purpose of this model was to predict cable conductor temperature fluctuations over time given current loading.

Previously, the Bureau had conducted extensive research to determine the relationship between current load and temperature rises in coal mine trailing cables (*2*). Portable power cables were continuously and periodically loaded with direct current of various magnitudes. Temperature rises within and on the cables were measured with thermocouples and the data were recorded by computer. A typical steady state test result is shown in figure 5.

A literature search (*17*) revealed that, neglecting radiation and changes in conductor resistance, cable temperatures should rise and fall exponentially according to the following relationship:

$$T = (T_i - T_f)\, e^{\frac{(-t)}{\tau}} + T_f, \qquad (13)$$

where T = cable temperature rise above ambient at the end of time interval t, °C,

T_i = initial temperature rise at the start of that interval, °C,

T_f = final, stabilized temperature rise, °C,

t = time, s,

and τ = thermal time constant, s.

The thermal time constant represents a ratio of system heat capacity to the rate of heat transfer from the system. During heating, for example, the constant is equal to the time required to reach 63% of the final temperature rise. Thermal time constants are influenced by three factors: (1) the volume-to-surface area ratio or cable geometry; (2) the product of the density and specific heat of the cable, thermodynamic properties; and (3) the convective heat transfer coefficient, or the rate at which heat is removed from the cable surface.

The empirical model incorporated the steady state load test results for three round and three flat G-GC cables ranging from a fraction to up to 150% of rated ampacity (*18*). In constructing the model, the relationship between stabilized conductor temperature rise and constant load current was initially established for each cable by fitting functions of the form $y = ax^b$ to the test data using commercial data analysis software (fig. 6). Through

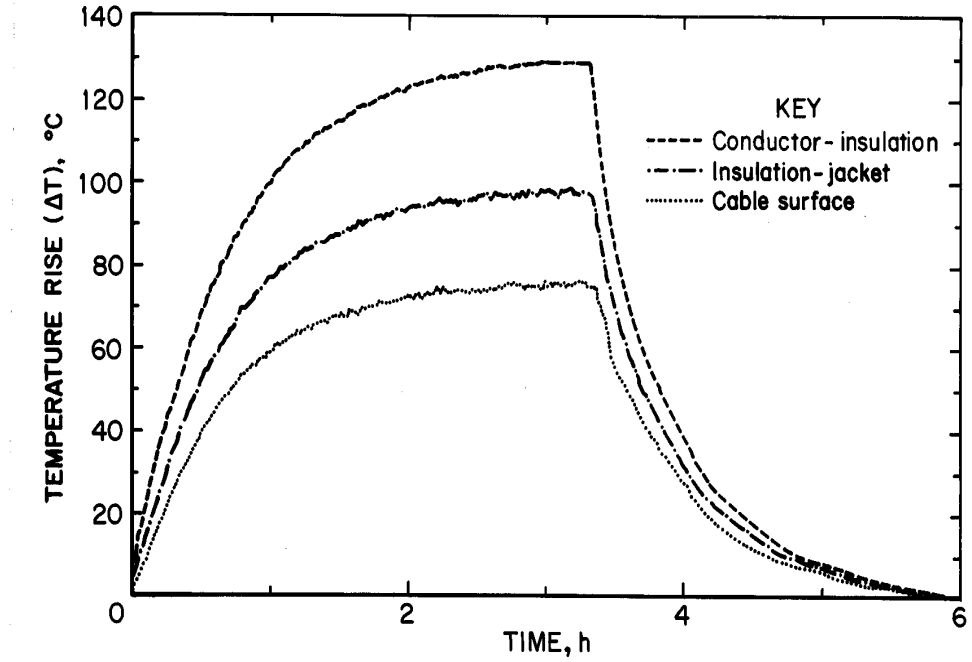

Figure 5.—Measured temperature rise in #2/0 AWG, 3/C, round, G-GC cable loaded at 400 A.

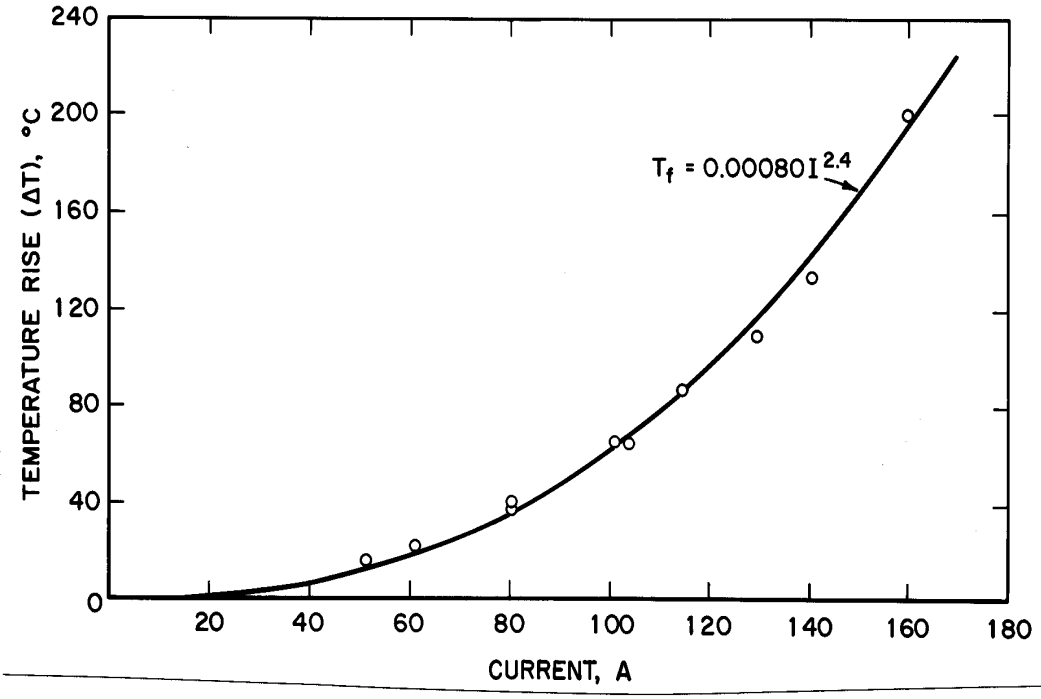

Figure 6.—Temperature rise versus current in #6 AWG, 3/C, round, G-GC cable.

interpolation, the current yielding the 70° C temperature rise, i.e., rated ampacity, was determined for each cable. These rated currents for a 20° C ambient were found to be 13% to 30% greater than those specified by ICEA (*18*). A plot of these rated currents versus cable size (fig. 7) shows that flat cables should have a higher current rating or ampacity than the same size round cable. This finding is not consistent with mine trailing cable ampacity tables (*18*), in which flat and round unshielded cables are lumped together. In all likelihood, the flat configurations, with 25% greater surface area for a given wire size, facilitate heat transfer to air. Interestingly, when the curves showing final temperature rise versus current are normalized to the rated ampacity for each cable, the data points become tightly clustered. This gives rise to a relationship where the temperature rise for any cable in the #6 to #4/0 range can be described as a function of the percent rated ampacity (fig. 8).

Next, equation 13 was fitted separately to the heating and cooling portions of the averaged conductor temperature curves (fig. 5) to obtain thermal time constants of heating and cooling. The heating constants were found to be independent of current load (fig. 9), while the cooling constants, calculated under no load, varied inversely with initial temperature (fig. 10). Since the cooling constant calculations were made with a preheated cable, this slight inverse relationship was attributed to radiation effects, which were neglected in equation 13. Multiple regression techniques were then employed to adapt the model to any size G-GC cable within the range of #6 to #4/0 AWG. Comparisons were made between simulated loads and actual load tests to gauge model accuracy. Figure 11 depicts model output and an actual load test for the #4/0 AWG cable carrying 300 A, 60% of the time.

This model was then incorporated into an interactive computer program that displays conductor temperature given an arbitrary current load determined by the user. The program consists of a series of menu screens, which are depicted in the appendix. To begin, the user specifies the cable to be evaluated. Next, the simulated load is defined. This may be the prior simulation, which is useful in comparing the thermal performance of differing cable sizes or shapes. The user is then given the choice of defining the hypothetical electrical load as a series of current-time intervals or as a repeatable or cyclic load. Another option is to read into the program an actual load current from a data file. The program output displays cable conductor temperature rise over time with the current load superposed (appendix).

This program is useful in several respects. It can be utilized by designers and approvers of new mining machines to determine the cable temperatures to be anticipated given the machine load cycle. Comparisons among various sizes can facilitate selection of the appropriate cable and ensure maximum safety and efficiency. It should be emphasized that the program provides no safety factor; the temperatures predicted are those that would be expected from a given input current. Users may want to incorporate an appropriate safety factor. Further, the program could be interfaced with hardware to monitor machine currents in real time and predict cable conductor temperatures. This information could be stored to provide a history of machine and cable usage. Ultimately this program could be the basis for a cable protection system. In its present form the program can provide a measure of conductor insulation deterioration through integration of time and temperature data. However, to offer more comprehensive protection it should be responsive to transient overcurrents. Accordingly, laboratory tests were conducted to evaluate the thermal performance of overloaded trailing cables.

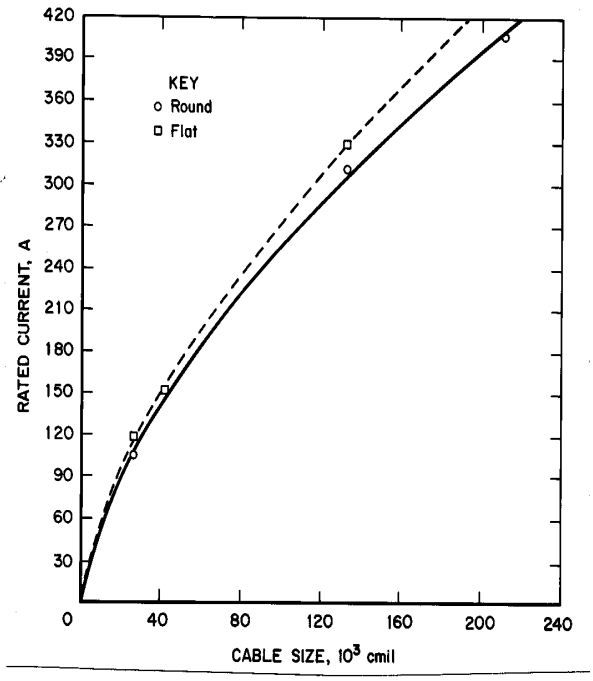

Figure 7.—Rated currents for flat and round configurations.

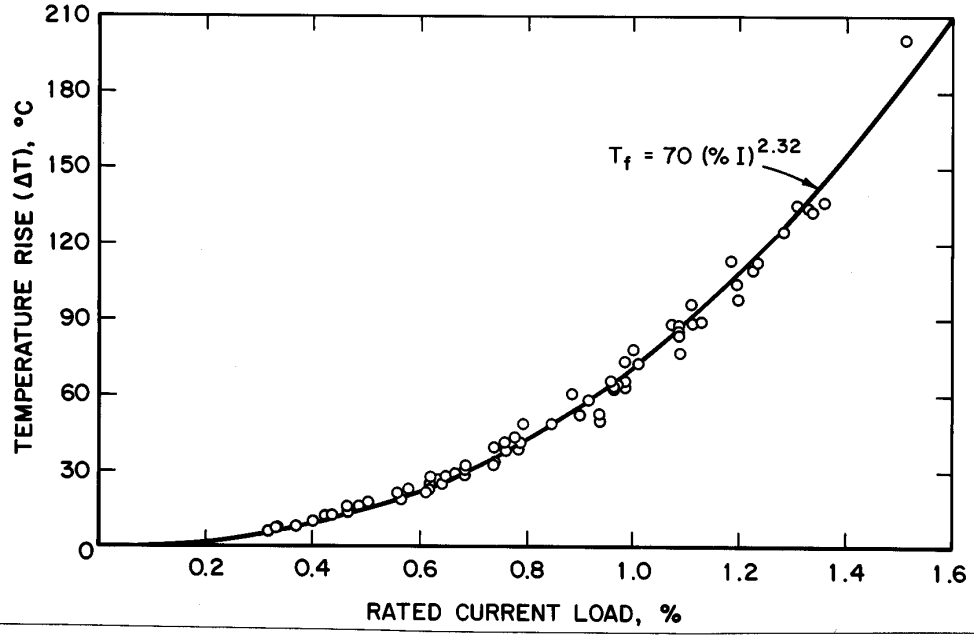

Figure 8.—Conductor temperature rises and percent rated load.

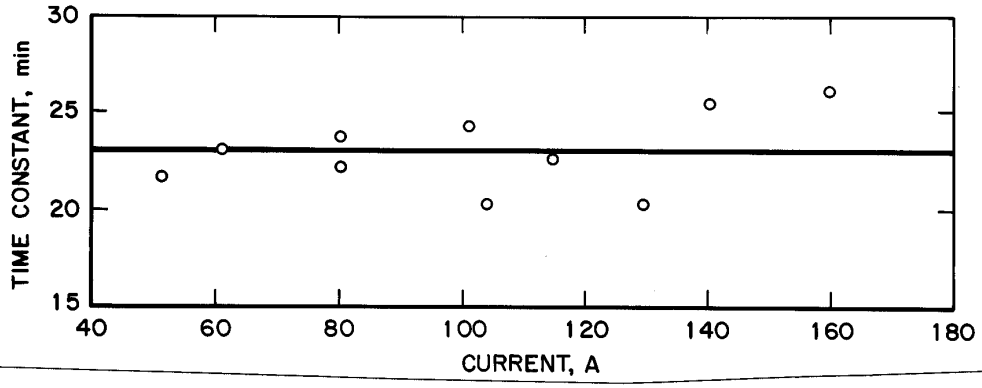

Figure 9.—Heating time constant versus current for #6 AWG, 3/C, round, G-GC cable.

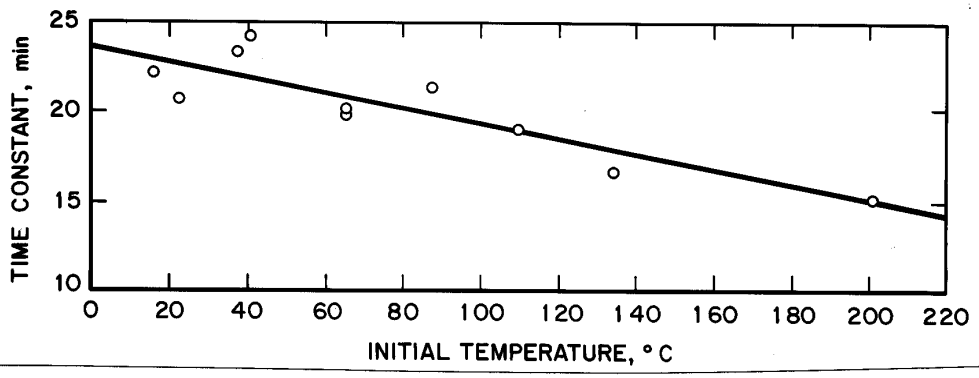

Figure 10.—Cooling time constant versus initial temperature in #6 AWG, 3/C, round, G-GC cable.

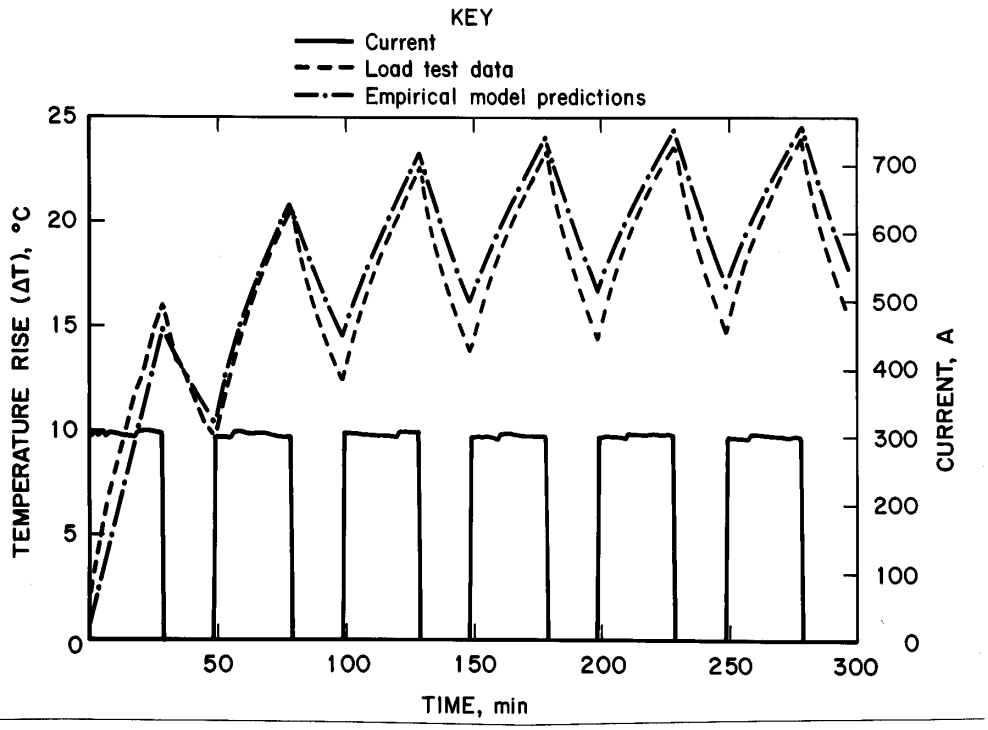

Figure 11.—Comparisons of actual load test results with empirical model predictions for #4/0 AWG, 3/C, round, G-GC cable.

OVERLOAD TESTS

In laboratory load tests, drag cable samples were subjected to relatively long-duration overcurrents ranging from 2 to 12 times the cable's rated 90° C ampacity. The test setup, essentially identical to that used previously in steady state and periodic load tests (*2*), will be summarized here.

The cables were suspended horizontally by rope 3 ft above and parallel to the lab floor. The test site ambient was maintained at 20°±2° C. Air currents in the vicinity of the cable from forced room ventilation ranged from 0 to 1 fps. All load tests were conducted using single-phase alternating current. Test currents less than 2,250 A were obtained from the three-phase supply of a motor test station in the Mine Electrical Laboratory at the Bureau. Above this level, a high-current step-down welding transformer was utilized as the power source. Type T thermocouples (#24 AWG, insulated with Teflon fluorocarbon polymer) with accuracies of ±0.5° C or 0.4% of reading, whichever was greater, were employed to measure temperatures within and on the cable. The thermocouples were in turn connected to a 32-channel datalogger that was programmed to read and transmit data to a personal computer. Commercial data acquisition software was used to collect the data, display them in real time, and store them on a disk (fig. 12).

The overload test currents were automatically interrupted when the temperature at any of the 30 monitored cable locations approached the range where the EPR insulation could be thermally damaged (170° to 210° C). This was accomplished by connecting the datalogger relay circuit to either the trip contacts of a molded-case circuit breaker inserted in series with the cable conductors or the emergency stop contacts of the high-current welding transformer. A constant current controller automatically adjusted the power source output voltage to compensate for changes in conductor resistance during conductor heating. Sampling rates ranged from 1 min for light overloads to 2 s at 1,200% ampacity.

Typical load test results are shown in figures 13 and 14 for the #2/0 AWG round cable. Test duration varied inversely with current. For example, with a 200% overload (fig. 13) it took about 27 min for the conductor to achieve a 150° C temperature rise, while at 11 times ampacity (fig. 14) the conductor reached this level in 25 s. An interesting phenomenon was observed at the conductor-insulation, insulation-jacket, and cable surface-air interfaces. At light overloads, these locations appeared to reach a maximum temperature nearly simultaneously, temperature rise at the surface being roughly half that at the

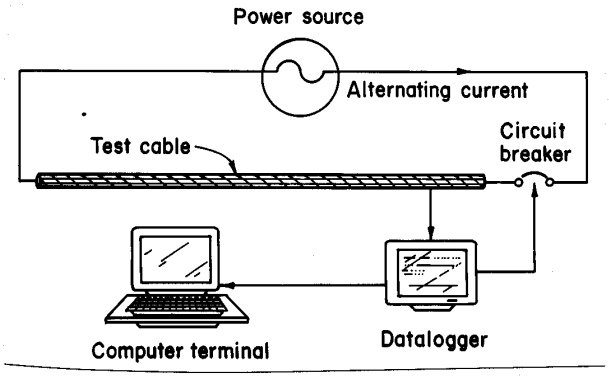

Figure 12.—Overload test setup.

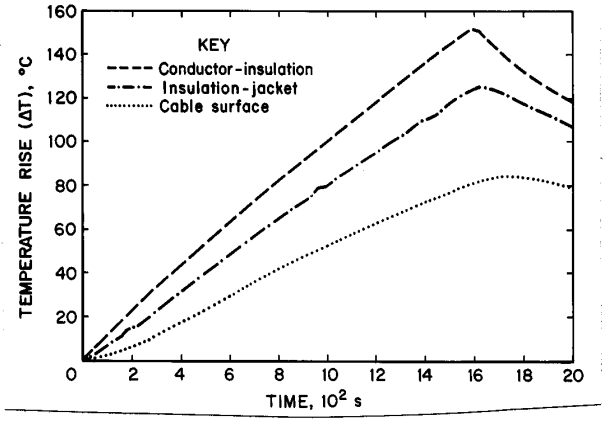

Figure 13.—Light (200% rating) overload on #2/0 AWG, 3/C, round, G-GC cable.

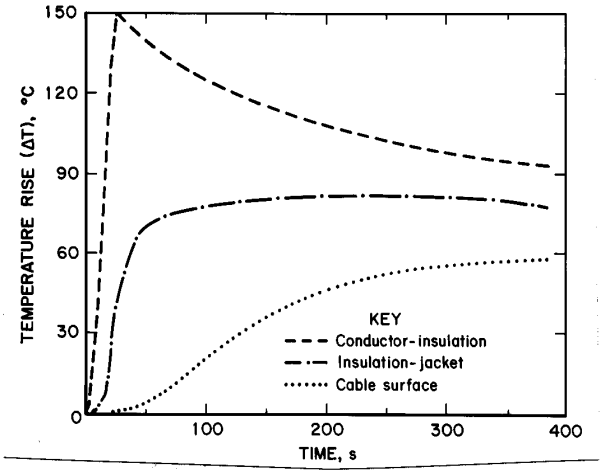

Figure 14.—Heavy (1,100% rating) overload on #2/0 AWG, 3/C, round, G-GC cable.

conductor-insulation interface. However, with heavier overloads, when the conductor temperature peaked, the temperature of the surface was barely elevated above the lab ambient. In fact, as shown in figure 14, temperatures at the surface reached a maximum 6 min after power was deenergized, and this maximum was only one-third the rise at the conductor-insulation interface. This delay in heat transfer from the conductor to the insulation, jacket, and eventually air means that cable jackets are stressed thermally to a relatively lesser degree during transient events than during loading near the cable's rated ampacity. Consequently, it is believed that the key to effective cable overload protection is the maintenance of conductor-insulation temperatures below the EPR damage threshold.

This "thermal inertia" is also manifested in the shape of the conductor temperature rise curve. At light overloads, this curve is an ascending exponential typical of those at or below rated ampacity (equation 13). At high overloads, a double exponential characteristic shape is apparent (fig. 15). This is important from a thermal modeling standpoint, as equation 13 can no longer be used to accurately predict temperature rise over time. Rather, the overload thermal rise curve seems to be a combination of equations 1 and 13, the transition point occurring when heat buildup in the conductor begins to be transferred to the insulation. In fact, this delay in heat transfer probably happened in all cable load tests, but was not readily observed in tests at or near rated ampacities because of 1-min sampling rates (fig. 5). An attempt was made to mathematically account for this phenomenon by calculating the slope of both curves for a given current and time and executing a transition from equation 1 to equation 13 when the slopes equated. However, these calculations proved too unwieldy for inclusion in the thermal model.

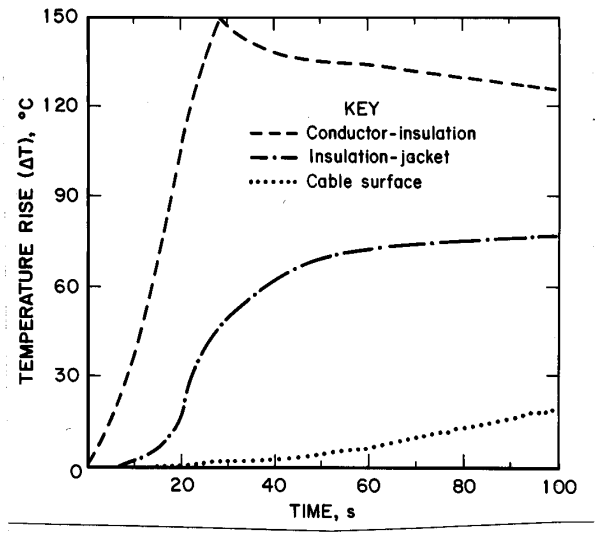

Figure 15.—Heavy (1,100% rating) overload on #2/0 AWG, 3/C, round, G-GC cable with time scale expanded.

IEEE Standard 242 (*8*) represents the overload region with the following relationship:

$$\frac{I_o}{I_n} = \sqrt{\frac{\frac{T - T_a}{T_n - T_a} - \left(\frac{I_i}{I_n}\right)^2 e^{-t/K}}{1 - e^{-t/K}}} \left(\frac{230 + T_n}{230 + T}\right), \quad (14)$$

where I_o = overload current,

I_n = normal current rating,

T = conductor temperature,

T_n = normal cable temperature rating,

T_a = ambient temperature,

I_i = initial current prior to overload,

t = time of overload,

and K = a constant, dependent on cable size and configuration.

However, the assumptions used to derive this equation are the same ones used for equation 13, namely that radiation and changes in conductor resistance are neglected. Consequently, equation 14 cannot be used to accurately predict conductor temperatures rises over time during cable overloads.

CONCLUSIONS

The thermal performance of both flat and round type G-GC portable power cables under normal loading circumstances has been successfully modeled empirically. An alternate mathematical model also yielded reasonable predictions of the stabilized conductor temperature rise for round cables. The temperature prediction technique of the empirical model utilized a somewhat simplistic approach, assuming an exponential rise and fall in conductor temperatures over time in response to step changes in load currents. Realistic model parameters were derived from extensive load tests of cables at or near rated current carrying capacity. A key finding of this analysis was that flat cables have a higher current rating or ampacity than the same size round cable. Additional laboratory tests were then conducted to measure temperature rises in cables energized with overcurrents in hopes of incorporating the thermal response of cables under such overloads into the thermal model. However, efforts to expand the scope of the empirical model into the overload range were not successful.

Nonetheless, the value of the existing thermal model should not be underestimated. In the form of an interactive computer program, it can be used by designers and approvers of new mining machines to determine the cable temperatures to be anticipated given the machine load cycle. Comparisons among various sizes and types can facilitate selection of the appropriate cable size while ensuring maximum safety and efficiency. In addition, the program can be interfaced with hardware to monitor machine currents in real time and predict cable conductor temperatures. This information could then be stored to provide a history of machine-cable usage.

RECOMMENDATIONS FOR FUTURE RESEARCH

As stated previously, the value of the thermal model as a protection methodology would be augmented if its application range were extended beyond normal cable loading. Since efforts to amplify the empirical model proved unsuccessful, a reevaluation of the mathematical model may be warranted. Specifically, the assumption of a uniform temperature across the single lumped metallic conductor should be investigated further. In addition, adjustments may be necessary for the assumed jacket emissivity and convective heat transfer coefficient. The resultant mathematical model would be more complex than the existing empirical model (a separate theoretical analysis for flat cable configurations would be still more complicated). However, these mathematical approaches do have the enhanced capability of predicting temperatures under any loading conditions, including overloads.

If conductor temperatures can be successfully predicted for abnormal as well as normal load conditions, the next logical step is to incorporate this into a cable protection system. Overloaded cables may attain high temperatures that can damage cable insulation. Consequently, the electrical current must be interrupted promptly to preclude this potential hazard. However, this must not occur so quickly as to cause nuisance tripping of the cable

protection system or to preclude efficient operation of the cable. To accurately match protection operating characteristics to cable thermal performance, the limits of insulation thermal damage must be defined for overloads. This can be accomplished by extending the previously derived (*10*) Arrhenius plots for EPR insulation in the high temperature range. Allowable time-current combinations can then be derived by adding appropriate safety factors.

It is envisioned that any computer-based cable protection system would augment existing short circuit protection in the form of fuses and/or circuit breakers. Thus, at currents above motor or transformer inrush, the present protective devices would activate with no intentional time delay.

REFERENCES

1. Hansloven, J. J. Trailing Cable Stresses in Underground Coal Mines. M.S. Thesis, PA State Univ., University Park, PA, 1978, 275 pp.

2. Yenchek, M. R., and P. G. Kovalchik. Thermal Characteristics of Energized Coal Mine Trailing Cables. IEEE Trans. Ind. Appl., v. 25, No. 5, Sept./Oct. 1989, pp. 824-829.

3. ____. Thermal Characteristics of Energized Shielded and Reeled Trailing Cables. IEEE Trans. Ind. Appl., v. 27, No. 4, July/Aug. 1991, pp. 791-796.

4. Kaufmann, R. H. Selecting Power Cables To Meet Short Circuit Requirements. Power Gener. and Power Plant Eng., v. 53, No. 2, Feb. 1949, pp. 64-67.

5. Insulated Cable Engineers Association (South Yarmouth, MA). Short-Circuit Characteristics of Insulated Cable. ICEA Publ. No. P-32-382, 1987, 22 pp.; available from Natl. Electr. Manuf. Assoc., Washington, DC.

6. ____. Short-Circuit Performance of Metallic Shielding and Sheaths of Insulated Cables. ICEA Publ. No. P-45-482, 1987, 11 pp.; available from Natl. Electr. Manuf. Assoc., Washington, DC.

7. Jones, B. W., and J. A. Scott. Short-Time Current Ratings for Aircraft Wire and Cable. AIEE Trans., v. 65, Oct. 1946, pp. 644-648.

8. Institute of Electrical and Electronic Engineers (New York). IEEE Recommended Practice for Protection and Coordination of Industrial and Commercial Power Systems. ANSI/IEEE Stand. 242, 1986, p. 344.

9. Lazar, I. New Insulation Developments for Electrical Wire and Cable. Specifying Eng., Sept. 1981, pp. 90-93.

10. Yenchek, M. R., and P. G. Kovalchik. Mechanical Performance of Thermally-Aged Trailing Cable Insulation. IEEE IAS Trans., v. 25, No. 6, Nov./Dec. 1989, pp. 1000-1005.

11. Yenchek, M. R., and P. G. Kovalchik. The Impact of Current Load on Mine Trailing Cable Thermal Life. Paper in Conference Record of the 10th WVU International Mining Electrotechnology Conference. WV Univ., Morgantown, WV, July 1990, pp. 17-22.

12. U.S. Code of Federal Regulations. Title 30—Mining Resources; Chapter I—Mine Safety and Health Administration, Department of Labor; Subchapter O—Coal Mine Safety and Health; Part 75—Mandatory Safety Standards—Underground Coal Mines; Section 75.601; July 1, 1989.

13. Fesak, G., W. S. Vilcheck, W. J. Helfrich, and D. C. Deutsch. Instantaneous Circuit Breaker Settings for the Short Circuit Protection of Three-Phase 480-, 600-, and 1040-V Trailing Cables. IEEE Trans. Ind. Appl., v. IA-17, No. 4, July/Aug. 1981, pp. 369-376.

14. Vilcheck, W. S., G. Fesak, and W. J. Helfrich. Instantaneous Circuit Breaker Settings for the Short-Circuit Protection of Direct Current 300- and 600-V Trailing Cables. IEEE Trans. Ind. Appl., v. IA-17, No. 4, July/Aug. 1981, pp. 362-368.

15. Luxbacher, G. W. Evaluation of the Effectiveness of Molded-Case Circuit Breakers for Trailing Cable Protection. Ph.D. Thesis, PA State Univ., University Park, PA, Nov. 1980, p. 128.

16. Ames, W. F. Numerical Method for Partial Differential Equations. Barnes and Noble, 1969, pp. 52-53.

17. Graham, R. C. Overload Classification for Secondary Network Cables. AIEE Trans., v. 74, Pt. III-PAS, Oct. 1955, pp. 916-919.

18. Insulated Cable Engineers Association (South Yarmouth, MA). Ethylene-Propylene-Rubber-Insulated Wire and Cable for the Transmission and Distribution of Electrical Energy. Pt. 8 (appendices). ICEA Publ. S-68-516, 1985, p. 8; available from Natl. Electr. Manuf. Assoc., Washington, DC.

APPENDIX.—EMPIRICAL MODEL MENUS

A series of menu screens from the interactive computer program is shown, ultimately displaying cable conductor temperature rise over time with the current load superposed.

CABLE SPECIFICATION

0. #6 AWG, 3/c, G-GC.	5. #1 AWG, 3/c, G-GC.
1. #5 AWG, 3/c, G-GC.	6. 1/0 AWG, 3/c, G-GC.
2. #4 AWG, 3/c, G-GC.	7. 2/0 AWG, 3/c, G-GC.
3. #3 AWG, 3/c, G-GC.	8. 3/0 AWG, 3/c, G-GC.
4. #2 AWG, 3/c, G-GC.	9. 4/0 AWG, 3/c, G-GC.

Current Selection is: 1
Current Shape is : ROUND

Press 'Q'	To QUIT Simulation
0-9	To SELECT Cable NUMBER.
'RETURN'	To CONTINUE to Duty Screen.
'R' or 'F'	To SELECT the Cable SHAPE.

CURRENT DUTY CYCLE

Please choose method of Duty Cycle Definition

1 REUSE Last Duty Cycle Input.
2. Input Duty Cycle as a Series of INTERVALS.
3. Define SUBINTERVAL to be Used Multiple Times.
4. Read in Duty Cycle from a FILE.

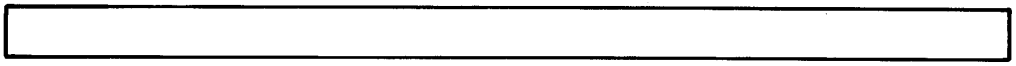

INTERVAL DEFINITION

Enter the SAMPLE Rate (Seconds): 60_ [Default = 30]
Enter the number of INTERVALS : 4_ [Default = 1]

DURATION of Interval #2 ?

Hours : 2_ Min: 30 Sec: 00
CURRENT Level (Amps): 130_

SUBINTERVAL DEFINITION

Enter the SAMPLE Rate (Seconds): 60_ [Default = 30]

Enter the ON TIME: Hours: 00 Min: 45 Sec: 00
Enter On Time CURRENT LEVEL (Amps): 200_

Enter the OFF TIME: Hours: 00 Min: 15 Sec: 00

How many times to REPEAT Subinterval 8_ [Default = 10]

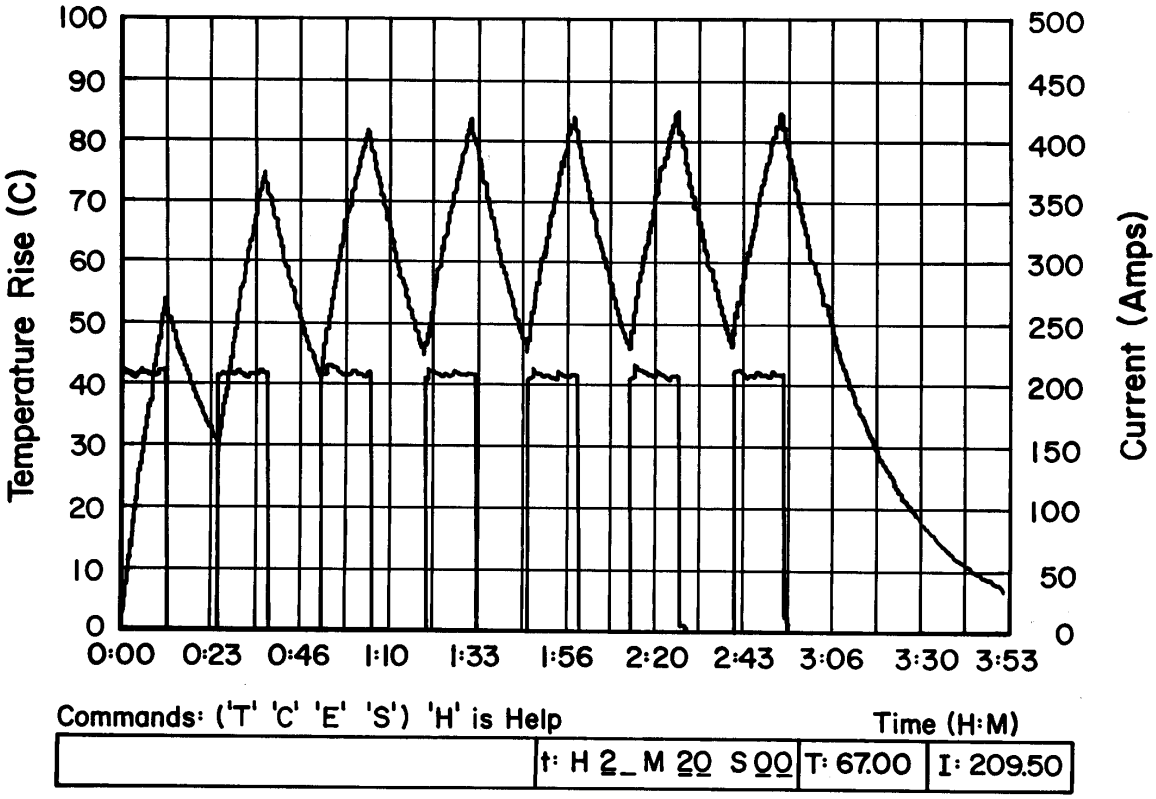
Temperature Rise (C)
100
90
80
70
60
50
40
30
20
10
0
Current (Amps)
500
450
400
350
300
250
200
150
100
50
0
0:00 0:23 0:46 1:10 1:33 1:56 2:20 2:43 3:06 3:30 3:53
Commands: ('T' 'C' 'E' 'S') 'H' is Help
Time (H:M)
t: H 2_ M 20 S 00
T: 67.00
I: 209.50